

# Direct Observation of the Wheland Intermediate in Electrophilic Aromatic Substitution. Reversible Formation of Nitrosoarenium Cations

Stephan M. Hubig and Jay K. Kochi\*

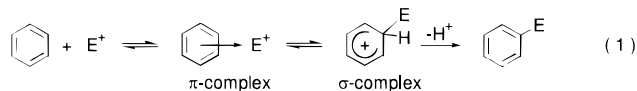
Contribution from the Department of Chemistry, University of Houston, Houston, Texas 77204-5641

Received April 14, 2000. Revised Manuscript Received June 21, 2000

**Abstract:** The Wheland intermediate in electrophilic aromatic nitrosation, viz. the nitrosoarenium  $\sigma$ -complex, is directly observed by transient absorption spectroscopy. Femtosecond time-resolved laser experiments based on charge-transfer photoexcitation of electron donor/acceptor (EDA) complexes of nitrosonium cation with various arenes reveal the ultrafast formation of nitrosobenzenium to occur in less than 10 ps via the radical/radical coupling of arene cation radicals and nitric oxide. The lifetimes of the  $\sigma$ -complexes in dichloromethane solution are strongly temperature dependent—varying from nanoseconds ( $T = 298$  K) to microseconds ( $T = 195$  K). Steady-state photolysis of arene/ $\text{NO}^+$  complexes in *n*-BuCl glasses at  $T = 77$  K leads to nitrosoarenium  $\sigma$ -complexes which persist for several hours. Based on a reaction scheme that includes an ultrafast equilibrium between the  $[\text{ArH}^+, \text{NO}^*]$  radical pair and the nitrosoarenium  $\sigma$ -complex, energy diagrams are constructed which establish the highly endergonic reaction profile of electrophilic aromatic nitrosations with the arene/nitrosonium  $\pi$ -complex as the thermodynamic sink.

## Introduction

Electrophilic aromatic substitutions are commonly considered to occur via transient  $\pi$ - and  $\sigma$ -complexes as sequential intermediates,<sup>1</sup> i.e.,



In fact, numerous  $\pi$ -complexes of arenes with electrophiles have been observed during substitution reactions due to their characteristic (charge-transfer) colors,<sup>2</sup> and many of them have been isolated in crystalline form and characterized by X-ray crystallography.<sup>3</sup> In contrast, the observation of  $\sigma$ -complexes, also known as Wheland intermediates, remains an experimental challenge owing to their generally ultrashort lifetimes which result in extremely low steady-state concentrations during the substitution reaction.<sup>4</sup> In general, such limitations in the detection of short-lived intermediates in thermal reactions are readily overcome if the reactive intermediates can be generated by photochemical means and thus observed by laser-flash photolysis techniques.<sup>5</sup> However, even time-resolved spectroscopic methods using ultrashort laser pulses have not been successfully applied to observe Wheland intermediates in aromatic nitrations in real time, which is due to their very fast deprotonation to form the nitroarene products.<sup>6,7</sup> On the other hand, the homologous hexaalkyl-substituted nitroarenium ions

(not easily deprotonated) are examples of persistent  $\sigma$ -complexes that were originally identified by Olah and co-workers via NMR spectroscopy at low temperature.<sup>4c,8</sup>

Aromatic nitrosations, as commonly carried out with nitrous acid generated in situ in acidic milieu,<sup>9</sup> are estimated to be  $> 10^{14}$  times less effective than the corresponding nitrations.<sup>10,11</sup> This difference in reactivity is generally attributed to a poorer electrophilicity of the nitrosating agents, viz., protonated nitrous acid and nitrosonium ( $\text{NO}^+$ ), as compared to the nitronium ion

(4) (a) Only hexasubstituted arenium  $\sigma$ -complexes such as chlorohexamethylbenzenium,<sup>4b-c</sup> nitrohexamethylbenzenium,<sup>4c-e</sup> heptamethylbenzenium,<sup>4f,g</sup> etc. have been characterized by NMR spectroscopy and/or X-ray crystallography. (b) Rathore, R.; Hecht, J.; Kochi, J. K. *J. Am. Chem. Soc.* **1998**, *120*, 13278. (c) Olah, G. A.; Lin, H. C.; Mo, Y. K. *J. Am. Chem. Soc.* **1972**, *94*, 3667. (d) Mamatyuk, V. I.; Rezvukhin, A. I.; Detsina, A. N.; Buraev, V. I.; Isaev, I. S.; Koptuyug, V. A. *Zh. Org. Khim.* **1973**, *9*, 2429. (e) See also: Koptuyug, V. A. *Top. Curr. Chem.* **1984**, *122*, 1. (f) Borodkin, G. I.; Nagi, S. M.; Gatilov, Y. V.; Shakirov, M. M.; Rybalvo, T. V.; Shubin, V. G. *Zh. Org. Khim.* **1992**, *28*, 1806. (g) Doering, W. von E.; Saunders, M.; Boyton, H. G.; Earhart, H. W.; Wadley, E. F.; Edwards, W. R.; Laber, G. *Tetrahedron* **1958**, *4*, 178. (h) Recently, protonated hexamethylbenzene, pentamethylbenzene, and mesitylene have been isolated as crystalline salts, and the structure of protonated pentamethylbenzenium has been determined by X-ray crystallography. See: Reed, C. A.; Fackler, N. L. P.; Kim, K.-C.; Stasko, D.; Evans, D. R.; Boyd, P. D. W.; Rickard, C. E. *J. Am. Chem. Soc.* **1999**, *121*, 6314.

(5) (a) We have demonstrated the power of time-resolved (laser) spectroscopy for the detection and identification of short-lived intermediates in various electrophilic aromatic substitution reactions including nitration,<sup>5b</sup> osmylation,<sup>5c</sup> mercuriation,<sup>5d</sup> etc. (b) Bockman, T. M.; Kochi, J. K. *J. Phys. Org. Chem.* **1994**, *7*, 325 and references therein. (c) Wallis, J. M.; Kochi, J. K. *J. Am. Chem. Soc.* **1988**, *110*, 8207. (d) Hubig, S. M.; Kochi, J. K. In *Electron Transfer in Chemistry*; Balzani, V., Ed.; Wiley-VCH: New York, in press.

(6) Olah, G. A.; Malhotra, R.; Narang, S. C. *Nitration: Methods and Mechanisms*; VCH: New York, 1989.

(7) The lack of deuterium isotope effects in the kinetics of nitrations confirms the fast deprotonation rates. See ref 6.

(8) See also Koptuyug et al. in refs 4d and 4e.

(9) Williams, D. L. H. *Nitrosation*; Cambridge University Press: Cambridge, 1988.

(10) Challis, B. C.; Higgins, R. J.; Lawson, A. J. *J. Chem. Soc., Perkin Trans. 2* **1972**, 1831.

(1) (a) Lowery, T. H.; Richardson, K. S. *Mechanism and Theory in Organic Chemistry*, 3rd ed.; Harper and Row Publishers: New York, 1987; p 623. (b) March, J. *Advanced Organic Chemistry*; John Wiley & Sons: New York, 1992; p 501.

(2) Rathore, R.; Kochi, J. K. *Adv. Phys. Org. Chem.* **2000**, *35*, 193.

(3) See, for example: (a) McMullan, R. K.; Koetzle, T. F.; Fritchie, C. *J. Acta Crystallogr.* **1997**, *B53*, 645. (b) Mascial, M.; Hansen, J.; Blake, A. J.; Li, W.-S. *Chem. Commun.* **1998**, 355. (c) Baysanov, A. S.; Crabtree, S. P.; Howard, J. A. K.; Lehmann, C. W.; Kilner, M. *J. Organomet. Chem.* **1998**, *550*, 59. (d) See also refs 2 and 15.



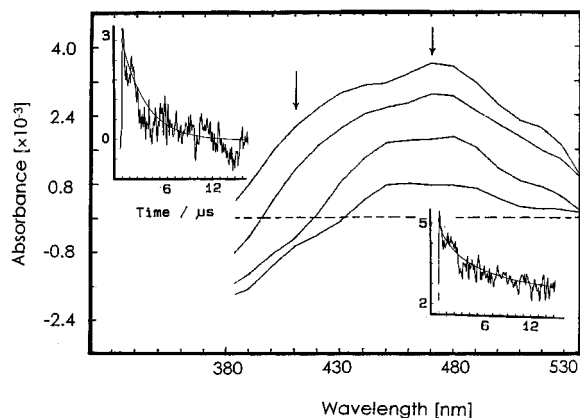


**Figure 1.** Transient absorption spectra obtained at 0.5, 1.5, 4.2, and 18  $\mu\text{s}$  (top to bottom) following the charge-transfer excitation of the mesitylene/ $\text{NO}^+$  EDA complex in dichloromethane at  $-60^\circ\text{C}$  with a 10-ns laser pulse at 355 nm. The spectra consist of the two overlapping absorption bands of mesitylene cation radical (centered at 470 nm) and nitrosomesitylenium cation (centered at 430 nm).

**Table 1.** Spectral and Kinetic Properties of Nitrosopolymethylbenzenium  $\sigma$ -Complexes<sup>a</sup>

Arene	$\lambda_{\text{max}}$ [nm] <sup>b</sup>		$\tau$ [ns] <sup>c</sup>	
	Cation Radical	$\sigma$ -Complex	T = 298 K	T = 195 K
1	440	430	<10	<sup>d</sup>
2	470	430	<sup>e</sup>	>3000
3	485	430	<4	100
4	490	430	<10	285
5	495	430	14	>2000

<sup>a</sup> In dichloromethane. <sup>b</sup> Absorption maximum. <sup>c</sup> Lifetime of the nitrosobenzenium  $\sigma$ -complex. <sup>d</sup> Not measured. <sup>e</sup> Solution thermally unstable at room temperature.

generated a transient spectrum which showed an absorption maximum at 470 nm and an additional strong absorption in the 380–450 nm range, peaking at 430 nm (see Figure 1). The 470-nm absorption band, which partially decayed on the 20- $\mu\text{s}$  time scale with mixed-order kinetics, was readily assigned to the mesitylene cation radical.<sup>24</sup> On the other hand, the absorption at 430 nm, which decayed completely to the baseline by first-order kinetics with a rate constant of  $k = 3 \times 10^5 \text{ s}^{-1}$ , clearly belonged to a different transient species. This transient was tentatively assigned to the nitrosomesitylenium  $\sigma$ -complex, i.e., the Wheland intermediate in the nitrosation of mesitylene.<sup>25</sup>

Similar transient spectra were obtained with other polymethylbenzenes such as *p*-xylene, durene, pentamethylbenzene, and hexamethylbenzene (see Table 1). Thus, the cation radicals of the alkyl-substituted benzenes exhibited absorption maxima at different wavelengths between  $\lambda_{\text{max}} = 440$  and 495 nm.<sup>26</sup> However, the overlapping absorption bands of the corresponding

(23) (a) Wynne, K.; Galli, C.; Hochstrasser, R. M. *J. Chem. Phys.* **1994**, *100*, 4797. (b) Asahi, T.; Mataga, N. *J. Phys. Chem.* **1989**, *93*, 6575. (c) Hubig, S. M.; Bockman, T. M.; Kochi, J. K. *J. Am. Chem. Soc.* **1996**, *118*, 3842.

(24) Sehested, K.; Holcman, J.; Hart, E. J. *J. Phys. Chem.* **1977**, *81*, 1363.

(25) The preliminary assignment will be substantiated throughout this report by a thorough analysis of its spectroscopic and kinetic properties.

(26) For the absorption spectra of polyalkylbenzene cation radicals, see refs 21, 24, and 32 and references therein.

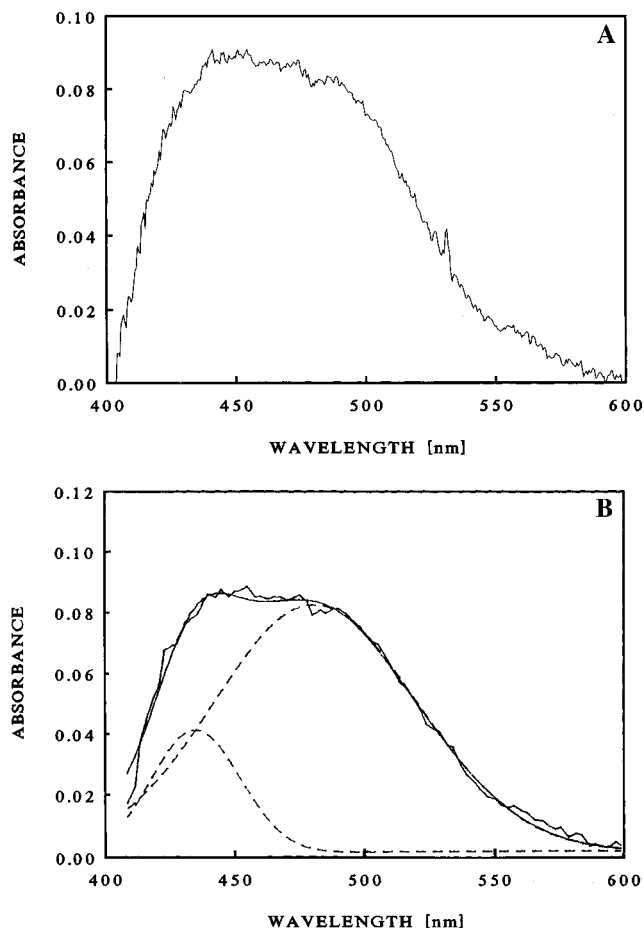


**Figure 2.** (A) Transient absorption spectrum obtained 25 ps upon charge-transfer (laser) excitation (at 355 nm) of the hexamethylbenzene/ $\text{NO}^+$  EDA complex in dichloromethane. (B) Deconvolution of the broad absorption band in (A) as two Gaussian absorption bands with maxima at 495 and 430 nm assigned to the hexamethylbenzene cation radical and the nitrosohexamethylbenzenium  $\sigma$ -complex, respectively.

$\sigma$ -complexes or Wheland intermediates appeared in identical positions and shapes with maximum at  $\lambda_{\text{max}} = 430 \pm 10 \text{ nm}$ . Importantly, the lifetimes of the nitrosobenzenium  $\sigma$ -complexes varied among the differently substituted benzene derivatives.  $\sigma$ -Complexes that could be observed at room temperature were generally short-lived. Nitrosopentamethylbenzenium and nitrosodurenium were short-lived even at low temperature (see Table 1). In contrast, the nitrosohexamethylbenzenium  $\sigma$ -complex was longer lived even at room temperature, and the solution did not react thermally or upon laser irradiation. Thus, we focus on this complex as a model to study the spectroscopic, kinetic, and thermodynamic properties of nitrosobenzenium  $\sigma$ -complexes in more detail.

**2. Spectroscopic and Kinetic Examination of the Nitrosohexamethylbenzenium  $\sigma$ -Complex.** Upon photoexcitation of the CT absorption bands of a ca. 0.5 mM solution of hexamethylbenzene/ $\text{NO}^+$  complex in dichloromethane with a 25-ps mode-locked Nd:YAG laser at either 355 nm (high-energy band) or 532 nm (low-energy band), a transient spectrum with a broad, flat absorption band was observed (see Figure 2A), which could be readily deconvoluted into two (Gaussian) bands with maxima at 430 and 495 nm, respectively (see Figure 2B). The 495-nm absorption band was readily ascribed to the hexamethylbenzene cation radical,<sup>24</sup> and the 430-nm band was assigned to the nitrosohexamethylbenzenium  $\sigma$ -complex.<sup>25</sup> Time-resolved spectroscopy at room temperature on the nanosecond time scale

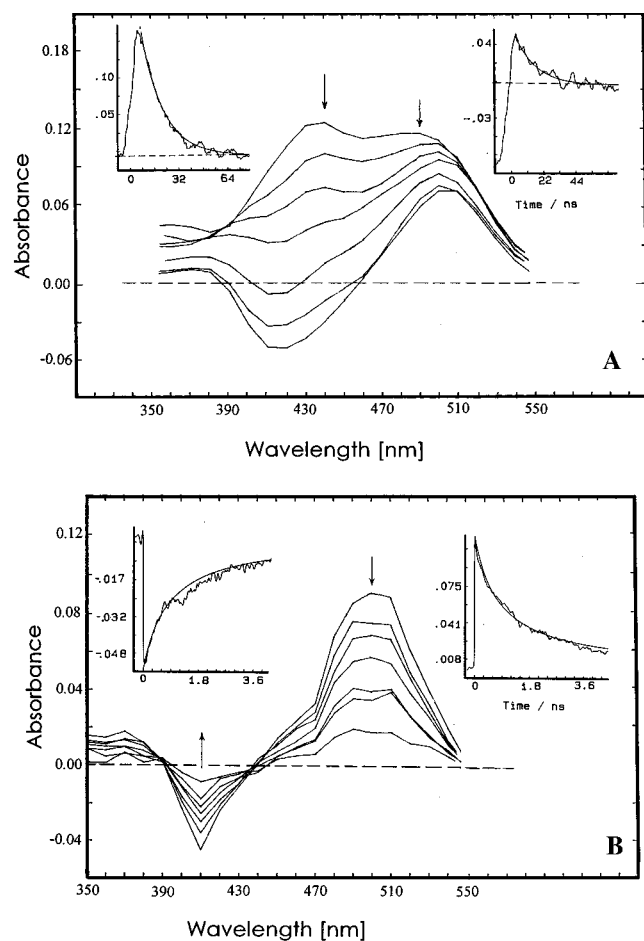


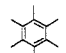
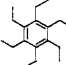
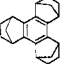
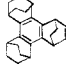
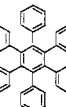
**Figure 3.** (A) First-order decay of the nitrosohexamethylbenzenium  $\sigma$ -complex at room temperature. [Spectra recorded at 13, 17, 21, 25, 32, 44, and 83 ns (top to bottom) upon 10-ns laser excitation.] (B) Subsequent second-order decay of the hexamethylbenzene cation radical (at 495 nm) and recovery of the ground-state charge-transfer absorption (at 400 nm). [Spectra recorded at 0.46, 0.67, 0.88, 1.7, 2.1, and 4.2  $\mu$ s upon laser excitation.]

(upon application of a 10-ns laser pulse of a Q-switched Nd:YAG laser at 355 nm) revealed a kinetic behavior similar to that observed with mesitylene at low temperature (vide supra). Thus, the  $\sigma$ -complex decayed completely within 40 ns with a first-order rate constant of  $k = 7 \times 10^7 \text{ s}^{-1}$ , whereas the absorption band of the hexamethylbenzene cation radical at 495 nm remained more or less unchanged over the same time span (see Figure 3A). The complete decay of the  $\sigma$ -complex resulted in a residual spectrum with the absorption band of the HMB cation radical at  $\lambda_{\text{max}} = 495 \text{ nm}$ <sup>24</sup> and a bleach of the CT absorption band around 400 nm. Both decayed on a longer (microsecond) time scale by second-order kinetics with diffusion-controlled rates<sup>27</sup> (see Figure 3B).

Similar transient absorption spectra on the picosecond and nanosecond time scales were obtained in chloroform and acetonitrile solutions. However, the lifetime of the  $\sigma$ -complex was significantly shorter in acetonitrile ( $\tau < 4 \text{ ns}$ ). Variation of the relative concentrations of HMB donor and  $\text{NO}^+$  acceptor from 30:1 to 1:20 in acetonitrile did not affect the relative absorptions of the  $\sigma$ -complex at 430 nm and the HMB cation radical at 495 nm.

(27) Diffusion-controlled reactions generally exhibit second-order rate constants of  $k \approx 10^{10} \text{ M}^{-1} \text{ s}^{-1}$ . See: Moore, J. W.; Pearson, R. G. *Kinetics and Mechanism*, 2nd ed.; Wiley: New York, 1981; p 239f.

**Table 2.** Spectral and Kinetic Properties of Hexaalkyl- and Hexaphenyl-Substituted Nitrosobenzium  $\sigma$ -Complexes<sup>a</sup>

	Arene	$\lambda_{\text{max}}[\text{nm}]^b$		$\tau [\text{ns}]^c$	
		Cation Radical	$\sigma$ -Complex	T = 298 K	T = 195 K
1		495	430	14	>2000
2		520	430	56	>2000
3		515	450	300	<sup>d</sup>
4		475	440	300	<sup>d</sup>
5		700	560	200	>2000

<sup>a</sup> In dichloromethane. <sup>b</sup> Absorption maximum. <sup>c</sup> Lifetime of the nitrosobenzium  $\sigma$ -complex. <sup>d</sup> Not measured.

**3. Other Hexasubstituted Benzene Donors.** Similar transient absorption spectra on the picosecond through microsecond time scales were observed upon CT excitation of EDA complexes of nitrosonium with various other hexaalkyl- or hexaphenyl-substituted benzenes (see Table 2) including hexaethylbenzene, hexaphenylbenzene, and two sterically hindered benzene donors (see entries 3 and 4). For hexaphenylbenzene, different transient spectra were obtained with a broad absorption band of the cation radical at 700 nm,<sup>28</sup> and the absorption of the  $\sigma$ -complex shifted to  $\lambda_{\text{max}} = 560 \text{ nm}$ .

**4. Temperature Effects.** When the nanosecond/microsecond time-resolved transient absorption spectra were recorded at various temperatures between 298 and 195 K, two temperature effects were observed. First, the relative intensities of the absorption bands of the cation radical and the  $\sigma$ -complexes changed dramatically. For example, upon lowering the temperature, the transient absorption spectra with hexamethylbenzene changed as follows. The absorption band centered at 430 nm became increasingly stronger as compared to that at 495 nm, ultimately leading to a spectrum at 195 K which consisted almost exclusively of the  $\sigma$ -complex and relatively little hexamethylbenzene cation radical absorption (see Figure 4). Second, the lifetime of the nitrosohexamethylbenzenium  $\sigma$ -complex increased by orders of magnitude on going from room temperature ( $\tau = 14 \text{ ns}$ ) to  $T = 195 \text{ K}$  ( $\tau > 1 \mu\text{s}$ , see Table 3).<sup>29</sup> Accordingly, the Arrhenius plot of the decay rate constants  $\ln k$  versus the reciprocal temperature yielded an activation energy of  $E_A = 7 \text{ kcal mol}^{-1}$  and a preexponential factor of  $A = 7 \times 10^{12} \text{ s}^{-1}$ . The Eyring evaluation led to a free activation enthalpy of  $\Delta G^\ddagger = 6.4 \text{ kcal mol}^{-1}$ . For hexaethylbenzene and hexaphenylbenzene, the Arrhenius evaluation of the temperature-dependent decay rates of the  $\sigma$ -complex yielded activation energies similar to those for hexamethylbenzene, but the frequency factors varied by 4 orders of magnitude (see Table 3).<sup>30</sup>

(28) The hexaphenylbenzene cation radical was also generated by electron-transfer quenching of photoexcited chloranil. Compare: Rathore, R.; Hubig, S. M.; Kochi, J. K. *J. Am. Chem. Soc.* **1997**, *119*, 11468.

(29) Note that the lifetime of the  $\sigma$ -complex was found to depend linearly on the HMB concentration. Thus, the decay rate constant changed by a factor of 10 on going from  $[\text{HMB}] \approx 2 \text{ mM}$  to 20 mM. Accordingly, a second-order rate constant for the HMB-assisted decay of nitrosohexamethylbenzenium was determined to be  $k_2 = 1 \times 10^8 \text{ M}^{-1} \text{ s}^{-1}$  at 195 K. Extrapolation to  $[\text{HMB}] = 0$  led to a lifetime of  $\tau = 20 \mu\text{s}$  at 195 K.

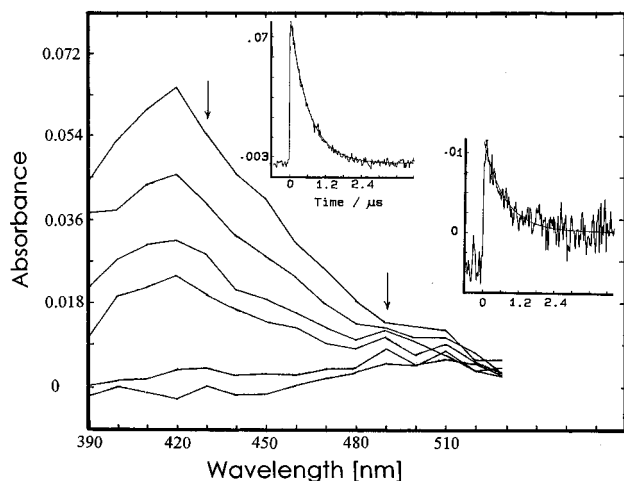


**Figure 4.** First-order decay of the nitrosohexamethylbenzenium  $\sigma$ -complex at  $T = 223$  K. [Spectra recorded at 0.77, 1.2, 1.4, 2.5, and 4.6  $\mu$ s upon 10-ns laser excitation at 532 nm.]

**Table 3.** Temperature Dependence of the Lifetime of Nitrosobenzenium  $\sigma$ -Complexes<sup>a</sup>

Arene	Temperature [K]	$\tau^b$ [ns]	$E_A (\Delta G^\ddagger)^c$ [kcal mol <sup>-1</sup> ]	$A^d$ [s <sup>-1</sup> ]
1	298	14	6.9 $\pm$ 0.1 (6.4)	7.5 $\times$ 10 <sup>12</sup>
	264	71		
	223	1000		
	208	1960 <sup>e</sup>		
2	298	56	4.0 $\pm$ 0.1 (3.7)	1.6 $\times$ 10 <sup>10</sup>
	288	71		
	273	91		
	253	156		
	233	345		
	203	1590		
3	298	200	3.0 $\pm$ 0.1 (2.5)	6.8 $\times$ 10 <sup>8</sup>
	273	430		
	250	670		
	238	910		
	223	1100		
	208	2130		

<sup>a</sup> In dichloromethane. <sup>b</sup> Lifetime of the  $\sigma$ -complex. <sup>c</sup> EA = activation energy,  $\Delta G^\ddagger$  = activation free enthalpy. <sup>d</sup> Frequency factor. <sup>e</sup>  $\tau > 20$   $\mu$ s for [HMB] = 0.29.

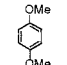
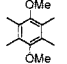
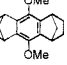
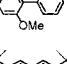
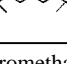
**5. Methoxy-Substituted Arenes and Naphthalene.** The first four entries in Table 4 show spectral and kinetic data for nitrosoarenium  $\sigma$ -complexes with methoxy substituents. Whereas the lifetimes of these transients at low temperatures did not differ significantly from those of alkyl-substituted nitrosobenzenium  $\sigma$ -complexes, the absorption maxima in the transient spectra were shifted in all cases to longer wavelengths (compare Tables 1, 2, and 4). Thus, the methoxy-substituted nitrosobenzenium ions showed absorption bands with maxima around 460–490 nm and tails extending beyond 550 nm. Similarly, the nitroso-naphthalenium  $\sigma$ -complex showed a strongly red-shifted absorption band with maximum at 570 nm (see Table 4).<sup>31</sup>

**II. Photogeneration of the  $\sigma$ -Complexes in a Butyl Chloride Matrix at 77 K.** The strong temperature effect on the decay rate constants (see Table 3) prompted us to examine

(30) We note that hexamethylbenzene showed a much weaker effect of the arene concentration on the rate constants for the decay of the  $\sigma$ -complex as compared to hexamethylbenzene.<sup>29</sup> Thus, the second-order rate constant for HEB-assisted decay of the  $\sigma$ -complex was calculated to be  $k_2 = 3 \times 10^6$  M<sup>-1</sup> s<sup>-1</sup> at  $T = 195$  K, which is 30 times slower than that of HMB.

(31) The nitroso-naphthalenium  $\sigma$ -complex was obtained by charge-transfer excitation of the naphthalene/NO<sup>+</sup> EDA  $\pi$ -complex which is stable at low ( $-78$  °C) temperatures.

**Table 4.** Spectral and Kinetic Properties of Methoxy-Substituted Nitrosobenzenium and Nitroso-naphthalenium  $\sigma$ -Complexes<sup>a</sup>

	Arene	$\lambda_{\max}$ [nm] <sup>b</sup>		$\tau$ [ $\mu$ s] <sup>c</sup>
		Cation Radical	$\sigma$ -Complexes	
1		430/460	460/530	3.6 <sup>d</sup>
2		495	465/570	2.5 <sup>e</sup>
3		485/515	485/530	1.1
4		590	520	0.025 <sup>f</sup>
5		620/680	570	g

<sup>a</sup> In dichloromethane. <sup>b</sup> Absorption maximum. <sup>c</sup> Lifetime of the nitrosoarenium  $\sigma$ -complex at  $T = 195$  K. <sup>d</sup>  $\tau = 16$   $\mu$ s for [DMB] = 0. Compare refs 29 and 30. <sup>e</sup> At  $T = 248$  K. <sup>f</sup> At  $T = 238$  K in acetonitrile. <sup>g</sup> Not measured.

the nitrosoarenium  $\sigma$ -complexes at liquid-nitrogen temperatures. *n*-Butyl chloride was chosen as the solvent for these experiments since it forms transparent glasses at  $T = 77$  K suitable for laser photolysis and UV/vis spectroscopic measurements.<sup>32</sup> First, the EDA complex of nitrosonium with hexamethylbenzene was prepared in *n*-butyl chloride solution and its concentration adjusted to reach an absorbance of about 0.5 at 532 nm. Charge-transfer (laser) excitation (at 532 nm) of the complex at room temperature resulted in transient absorption spectra very similar to those shown in Figures 2 and 3 for dichloromethane; the lifetime of the nitrosohexamethylbenzenium  $\sigma$ -complex was determined to be about 10 ns. Moreover, lowering of the temperature to  $T = 195$  K led to the same changes in the spectra and kinetics of the photogenerated transients as reported for dichloromethane solutions; i.e., the predominance of the  $\sigma$ -complex with a lifetime of about 1  $\mu$ s was observed.

Upon removal of the argon, the *n*-butyl chloride solution was cooled to  $T = 77$  K and the light brown solution turned into a dark purple/brown glass, the absorption spectrum of which showed the characteristic high-energy ( $\lambda_{\max} = 337$  nm) and low-energy ( $\lambda_{\max} = 500$  nm) CT bands of the EDA or  $\pi$ -complex of nitrosonium with the hexamethylbenzene donor.<sup>14,15</sup> Irradiation of the *n*-butyl chloride glass at  $T = 77$  K with either the second-harmonic (532 nm) or the third-harmonic (355 nm) output of a Nd:YAG laser resulted in the complete bleaching of the dark purple/brown color, and a persistent yellow color remained. The color changes with increasing number of incident laser pulses were followed spectroscopically on a (steady-state) spectrophotometer equipped with a quartz dewar containing liquid nitrogen. Thus, with extended exposure of the glass to laser irradiation, an increasing bleaching of the CT absorption bands at 337 and 500 nm and the growth of a new absorption between 400 and 500 nm were observed, which resulted in the formation of two isosbestic points (see Figure 5A). The difference spectra obtained either by subtraction of the spectra of irradiated and un-irradiated glass (see Figure 5B) or by pump-probe laser photolysis experiments (see Figure 5C) clearly revealed that the photogenerated yellow product showed an absorption spectrum identical to that of the  $\sigma$ -complex observed by transient spectroscopy (compare Figures 4 and 5).

(32) Shida, T. *Electronic Absorption Spectra of Radical Ions*; Elsevier: Amsterdam, 1988; p 19.

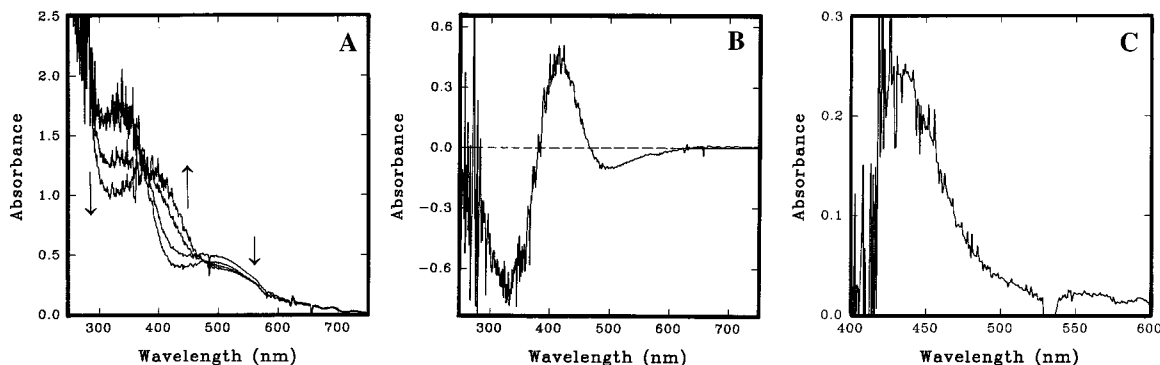


**Figure 5.** (A) Absorption spectra of the hexamethylbenzene/ $\text{NO}^+$  EDA complex in *n*-butyl chloride glass at  $T = 77$  K before and after exposure to 50, 100, and 400 laser pulses at 355 nm (1.5 mJ/pulse). (B) Change in absorbance between the first (0 pulses) and the last (400 pulses) spectrum in (A). (C) Difference absorption spectrum obtained upon charge-transfer excitation of the hexamethylbenzene/ $\text{NO}^+$  EDA complex in *n*-butyl chloride glass at  $T = 77$  K in a pump-probe laser experiment. The absorption bands centered at 430 nm in (B) and (C) are assigned to the nitrosohexamethylbenzenium  $\sigma$ -complex.

The yellow color persisted for hours at  $T = 77$  K. However, a slight increase of the temperature above the melting point of the butyl chloride glass ( $T > 150$  K) caused the yellow color to revert to purple/brown, and the spectrum of the molten glass was identical with the original CT spectrum prior to irradiation. As a result, multiple freeze-photolysis-thaw cycles could be carried out without any overall changes in the absorption spectra of the solution at room temperature. The color changes from purple/brown to yellow (at  $T = 77$  K) could also be achieved by irradiation with a pencil-style low-pressure mercury lamp with or without a 500-nm cutoff filter and even with a He/Ne laser at 633 nm (2 mW), which merely irradiates the extreme tail of the low-energy CT band.

Similarly, the yellow photoproduct was obtained upon 355-nm photolysis of the [HEB, $\text{NO}^+$ ] complex in *n*-butyl chloride glass at  $T = 77$  K. It could be repeatedly generated in freeze-photolysis-thaw cycles as described for hexamethylbenzene complexes (vide supra). Again, the spectrum of the stable yellow photoproduct at  $T = 77$  K closely matched that of the  $\sigma$ -complex observed at  $T = 195$  K (compare parts A and B of Figure 6).

Irradiation of the nitrosonium complex with a substituted naphthalene (see entry 5 in Table 4) in the *n*-BuCl matrix at  $T = 77$  K resulted in a photoproduct with the spectrum shown in Figure 7. This absorption spectrum with a maximum at 570 nm was identical with the spectrum of the nitrosonaphthalenium  $\sigma$ -complex obtained by transient spectroscopy at higher temperatures.

**III. The Kinetics for the Formation of the Nitrosoarenium  $\sigma$ -Complex.** Charge-transfer excitation of the polyalkylbenzene/ $\text{NO}^+$  complexes with a 25-ps laser pulse consistently resulted in the simultaneous formation of arene cation radical and  $\sigma$ -complex within the time period of the laser pulse (see, for example, Figure 2). Thus, to observe the interconversion between these two transients, a Ti:sapphire laser system with a 200-fs pulse at 400 nm was employed<sup>23c</sup> to improve the time resolution. As model system, we chose the hexamethylbenzene/ $\text{NO}^+$  complex because its solution in dichloromethane is stable at room temperature. The transient spectrum obtained 1 ps following the laser excitation showed a narrow absorption band with maximum at  $\lambda = 495$  nm which was readily assigned to the  $\text{HMB}^{+\bullet}$  cation radical. Subsequently, a broadening of this absorption band was observed over a time span of about 10 ps, ultimately leading to a broad, flat absorption band similar to that observed upon 25-ps excitation with the mode-locked Nd:YAG laser (compare Figures 2 and 8). Accordingly, the

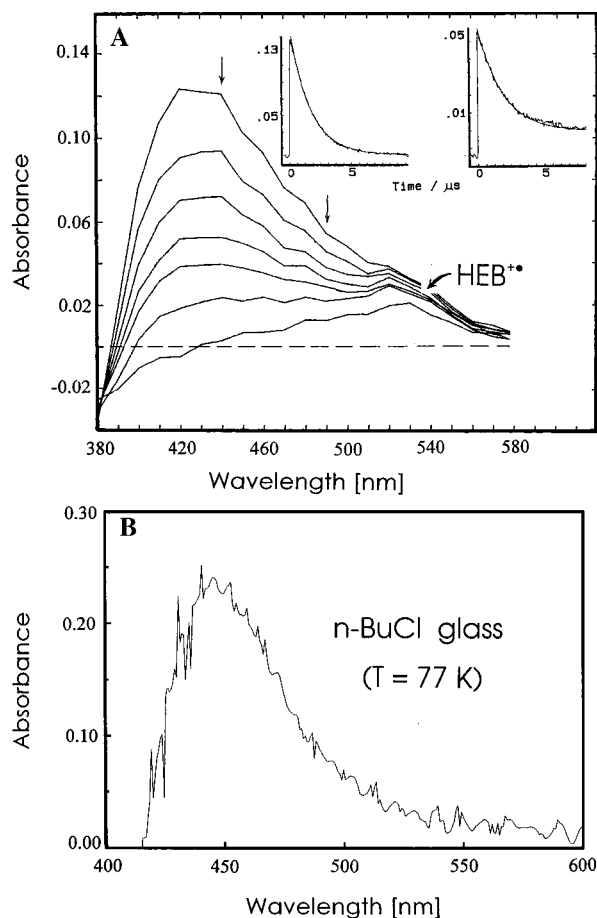


**Figure 6.** Absorption spectra of the nitrosohexaethylbenzenium  $\sigma$ -complex obtained upon charge-transfer excitation of the hexaethylbenzene/ $\text{NO}^+$  EDA complex at 355 nm (A) in dichloromethane at  $T = 195$  K and (B) in *n*-butyl chloride glass at  $T = 77$  K. The spectrum in (A) decayed within 10  $\mu\text{s}$ .

kinetic traces recorded at  $\lambda = 490$  and 440 nm revealed a slight decay of the hexamethylbenzene cation radical and the concomitant growth of the nitrosohexamethylbenzenium  $\sigma$ -complex, respectively (see Figure 9). Both the decay and the growth traces could be fitted to first-order kinetics with identical rate constants of  $k = 3 \times 10^{11} \text{ s}^{-1}$ .

Similar spectral changes on the early picosecond time scale were observed upon 200-fs laser excitation of the nitrosonium

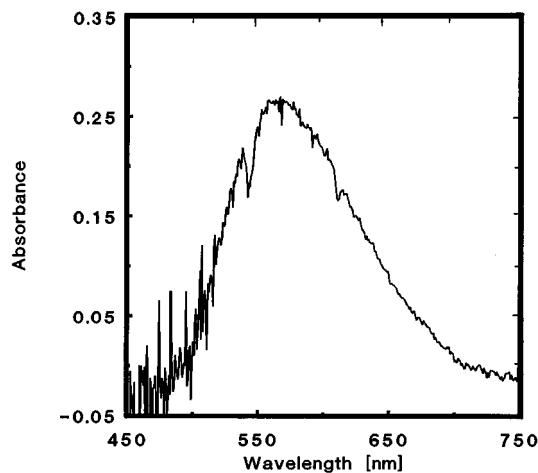


Figure 7. Absorption spectrum of nitrosonaphthalenium  $\sigma$ -complex in *n*-butyl chloride glass at  $T = 77$  K.

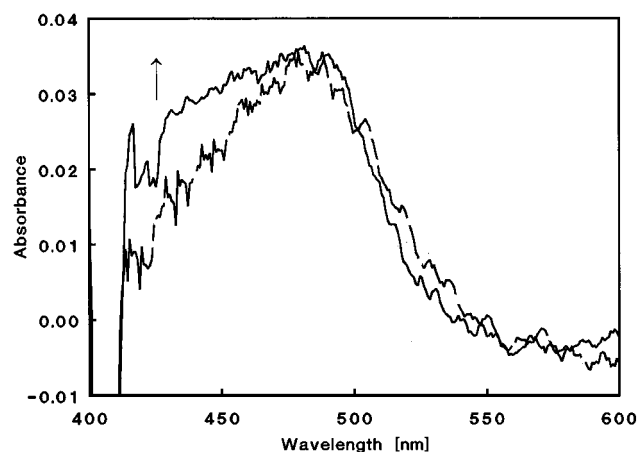


Figure 8. Transient absorption spectra obtained at 1 and 7 ps following the charge-transfer excitation (at 400 nm) of the hexamethylbenzene/ $\text{NO}^+$  EDA complex in dichloromethane with a 200-fs laser pulse at room temperature. The broadening of the absorption band in the 430-nm region is due to the ultrafast formation of the nitrosohexamethylbenzenium  $\sigma$ -complex.

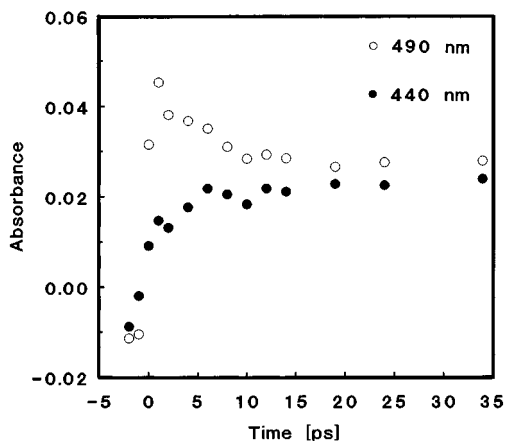


Figure 9. Kinetics of the ultrafast decay of hexamethylbenzene cation radical (monitored at 490 nm) and the formation of nitrosohexamethylbenzenium  $\sigma$ -complex (monitored at 440 nm) upon charge-transfer excitation of the hexamethylbenzene/ $\text{NO}^+$  EDA complex in dichloromethane with a 200-fs laser pulse at room temperature.

complex with pentamethylbenzene, and both femtosecond laser experiments clearly revealed the arene cation radical as the primary intermediate upon charge-transfer excitation.

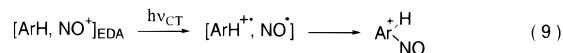
Table 5. Absorption Maxima ( $\lambda_{\text{max}}$ ) and Bandwidths ( $\Delta\nu$ ) of Various Hexamethylbenzenium Ions  $[\text{C}_6(\text{CH}_3)_6\text{E}]^+$  in Dichloromethane<sup>36</sup>

E	$\lambda_{\text{max}}$ (nm)	$\Delta\nu$ ( $\text{cm}^{-1}$ )	ref
H	$398 \pm 2$	3400	33
$\text{CH}_3$	$399 \pm 1$	2900	34
Cl	$410 \pm 2$	3200	4b
Br	$460 \pm 2$	3500	35
$\text{NO}_2$	$430 \pm 2$	3400	35
NO	$430 \pm 5$	2900	this work

Subsequently, the formation of the  $\sigma$ -complex from the cation radical was observed on the early picosecond time scale.

## Discussion

**I. Direct Observation and Identification of the Wheland Intermediate in Aromatic Nitrosation.** To substantiate the identity of the Wheland intermediate in nitrosation, viz., the nitrosoarenium  $\sigma$ -complex observed in the time-resolved and steady-state photolysis experiments of this study, let us summarize the important findings about its spectroscopic and thermodynamic properties as well as its formation and decay kinetics. First, we note that the Wheland intermediate is efficiently generated by charge-transfer irradiation ( $h\nu_{\text{CT}}$ ) of arene/ $\text{NO}^+$  EDA complexes. Since charge-transfer excitation of the EDA complex initially generates the arene cation radical,<sup>22,23</sup> the Wheland intermediate is formed in the subsequent coupling of arene cation radical with nitric oxide, i.e.,



The reaction sequence in eq 9 is unambiguously revealed in the femtosecond/picosecond time-resolved spectra recorded upon CT excitation of the  $\text{NO}^+$  complex of hexamethylbenzene (see Figures 8 and 9). Thus, we first obtain the absorption spectrum of the hexamethylbenzene cation radical which forms within the time period (200 fs) of the laser pulse. Subsequently, a partial decay of the cation radical and the concomitant formation of the nitrosohexamethylbenzenium  $\sigma$ -complex (with identical rates) are observed.

Second, the decay of the  $\sigma$ -complex results in the recovery of the original  $[\text{ArH}, \text{NO}^+] \pi$ -complex, as best demonstrated with the multiple freeze–photolysis–thaw cycles carried out in the *n*-butyl chloride glass. Moreover, the lifetimes of the  $\sigma$ -complexes are highly temperature dependent and vary from a few nanoseconds at room temperature to several hours at  $T = 77$  K. Accordingly, the Arrhenius and the Eyring evaluations result in activation energies and free activation enthalpies of up to 7 kcal  $\text{mol}^{-1}$  (see Table 3).

Third, the UV/vis absorption spectra of the nitrosoarenium  $\sigma$ -complexes closely resemble those of other  $\sigma$ -complexes. For example, a spectral comparison of various hexamethylbenzenium ions is given in Table 5, including protonated hexamethylbenzene,<sup>33</sup> heptamethylbenzenium,<sup>34</sup> and nitro-,<sup>35</sup> chloro-,<sup>4b</sup> and bromo-substituted<sup>35</sup> hexamethylbenzenium ions.<sup>36</sup> In particular, we note invariant wavelength positions and similar shapes (bandwidths) of the absorption bands of the nitroso- and

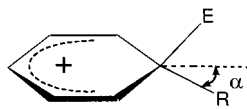
(33) (a) Kilpatrick, M.; Hyman, W. H. *J. Am. Chem. Soc.* **1958**, *80*, 77. (b) Deno, N. C.; Groves, P. T.; Saines, G. *J. Am. Chem. Soc.* **1959**, *81*, 5790.

(34) (a) See Rathore et al. in ref 4b. (b) See ref 4e, p 97.

(35) Dhanasekaran, T.; Kochi, J. K., unpublished results.

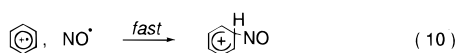
(36) For a detailed report on the spectroscopic properties (UV/vis,  $^1\text{H}$  NMR,  $^{13}\text{C}$  NMR) and X-ray structures of various hexamethylbenzenium ions, see: Hubig, S. M.; Kochi, J. K. *J. Org. Chem.*, in press.

the nitro-substituted  $\sigma$ -complexes (see entries 5 and 6 in Table 5).<sup>36</sup> Successful X-ray crystallography of the E = chloro, bromo, and methyl analogues show that the hexamethylbenzenium moieties have structural features that are also strikingly common: the skeletal structure showing close to  $C_{2v}$  symmetry, i.e.,



with all the carbon-carbon distances rather invariant with the *ipso*-substituent E.<sup>37</sup> We thus judge that the Wheland intermediates with E = NO and NO<sub>2</sub> also have the same basic structure.

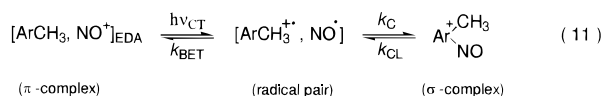
The spectroscopic, thermodynamic, and kinetic data presented in this work confirm the identity of the nitrosoarenium  $\sigma$ -complexes. These intermediates readily formed in the radical-radical coupling of the corresponding arene cation radicals with nitric oxide, i.e.,



In the case of mesitylene and xylene, these nitroso-substituted  $\sigma$ -complexes are the Wheland intermediates in nitrosation.<sup>14</sup> Moreover, the time-resolved studies which establish the formation of the nitrosobenzenium  $\sigma$ -complexes from the corresponding arene cation radicals represent the direct experimental verification of the reaction mechanism put forward in Scheme 1.<sup>14</sup> Accordingly, we now analyze the formation and decay kinetics of the nitrosoarenium ions in more detail. The temperature studies will provide thermodynamic data for energy diagrams, which will then be used to discuss the mechanism of aromatic nitrosation.

**II. The Reversible Formation of Nitrosoarenium and Its Temperature-Dependent Partitioning with the Arene Cation Radical.** The hexasubstituted arenes examined in this study play a key role in our understanding the formation and decay kinetics and energetics of nitrosoarenium ions since these substrates form  $\sigma$ -complexes with nitrosonium which cannot readily lose a proton to yield the corresponding nitrosoarene. As a result, the decay of hexasubstituted nitrosoarenium results in the complete recovery of the original arene/nitrosonium EDA complex. Since the generation of the nitrosoarenium  $\sigma$ -complex by CT photolysis of the EDA  $\pi$ -complex occurs in a two-step process via the arene cation-radical intermediate (vide supra), the simplest description of the formation and decay pathways of nitrosohexaalkylbenzenium includes a pair of reversible steps, as shown in Scheme 2, where  $k_{\text{BET}}$ ,  $k_{\text{C}}$ , and  $k_{\text{CL}}$  are the first-

### Scheme 2



order rate constants for back-electron transfer, coupling, and (homolytic) cleavage, respectively. Although this simple reaction sequence in Scheme 2 adequately describes the apparent reversibility of the  $\sigma$ -complex formation,<sup>38</sup> it does not account for the observation of long-lived arene cation radicals and

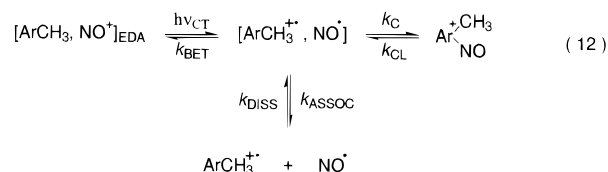
(37) (a) The carbon-carbon bond distances are almost identical (within  $3\sigma$ ). A small variation in the out-of-plane angle with  $\alpha = 55^\circ, 42^\circ$ , and  $55^\circ$  is observed for the chloro,<sup>4b</sup> bromo,<sup>37b</sup> and methyl analogues.<sup>4f,37b</sup> (b) Dhanasekaran, T.; Lindeman, S. V.; Kochi, J. K., unpublished results.

(38) We take the distinctive (temperature-dependent) spectral changes (compare, e.g., Figures 2 and 4) to reflect the reversible formation ( $k_{\text{C}}/k_{\text{CL}}$ ) of nitrosoarenium from the radical pair.

the temperature-dependent partitioning between them and the nitrosoarenium ions.

First, the long lifetimes of the arene cation radicals and their second-order decays on the microsecond time scale with diffusion-controlled rates<sup>27</sup> (see Figure 3B) clearly show that they exist as free, solvated ion radicals and not as ion-radical pairs as depicted in eq 11.<sup>39</sup> Second, the ultrafast ( $k \approx 10^{11} \text{ s}^{-1}$ ) formation of nitrosoarenium from the arene cation radical, its much slower ( $k \approx 10^7 \text{ s}^{-1}$ ) decay, and the comparable yields of both transients at room temperature (see Figure 2) cannot be reconciled with the simple reaction scheme in eq 11. Thus, an additional pathway must be included in the reaction scheme to account for the formation of solvated arene cation radicals by (reversible) dissociation ( $k_{\text{DISS}}$  and  $k_{\text{ASSOC}}$ ) of the  $[\text{ArCH}_3^{\bullet+}, \text{NO}^{\bullet}]$  radical pair,<sup>21,40</sup> as shown in Scheme 3. In

### Scheme 3



other words, the initially formed radical pair  $[\text{ArCH}_3^{\bullet+}, \text{NO}^{\bullet}]$  can either undergo back-electron transfer ( $k_{\text{BET}}$ ) to restore the original EDA complex, or dissociate ( $k_{\text{DISS}}$ ) to form solvated arene cation radicals and nitric oxide, or collapse ( $k_{\text{C}}$ ) to the nitrosoarenium  $\sigma$ -complex. The competition between these three pathways is confirmed experimentally by the quantum yields of less than unity for the formation of free solvated ion radicals which were reported previously.<sup>21</sup> Thus, free-ion yields as low as 0.1 have been found upon CT excitation of various polyalkylbenzene/NO<sup>+</sup> complexes, and the highest yield obtained for the HMB/NO<sup>+</sup> complex in various solvents does not exceed 0.7. These quantum yields of less than unity have been originally ascribed to the competition between back electron transfer ( $k_{\text{BET}}$ ) and dissociation ( $k_{\text{DISS}}$ ) of the radical pair  $[\text{ArCH}_3^{\bullet+}, \text{NO}^{\bullet}]$ .<sup>21</sup> In view of the new findings in this work, we must include the formation of nitrosoarenium. The limited quantum yields for free, solvated arene cation radicals are thus the result of the competition between back-electron transfer ( $k_{\text{BET}}$ ), reversible radical-pair collapse ( $k_{\text{C}}$  and  $k_{\text{CL}}$ ), and reversible dissociation ( $k_{\text{DISS}}$  and  $k_{\text{ASSOC}}$ ) in Scheme 3. However, since the back-electron transfer within the  $[\text{ArH}^{\bullet+}, \text{NO}^{\bullet}]$  radical pair exhibits pronounced inner-sphere character,<sup>21</sup> there is no clear-cut distinction between direct (inner-sphere) back-electron transfer ( $k_{\text{BET}}$ ) and the sequence of ultrafast radical-pair collapse ( $k_{\text{C}}$ ) followed by cleavage of the nitrosoarenium ( $k_{\text{CL}}$ ) combined with back-electron transfer. In other words, the formation of the nitrosoarenium  $\sigma$ -complex prior to back-electron transfer can be viewed as the classic case of an inner-sphere electron transfer in which the formation of a bonded precursor complex, i.e., nitrosoarenium, precedes the electron-transfer step.<sup>38</sup>

The reversible formation ( $k_{\text{C}}$  and  $k_{\text{CL}}$ ) of nitrosoarenium from the radical pair  $[\text{ArCH}_3^{\bullet+}, \text{NO}^{\bullet}]$  in Scheme 3 is strongly temperature-dependent, as demonstrated by the temperature dependence of the relative intensities of the absorptions of ion radicals and nitrosoarenium. Moreover, the fast, temperature-

(39) Back-electron transfer in ion-radical pairs follows first-order kinetics since no diffusional processes are involved.

(40) According to Scheme 3, the pathway for the decay of the nitrosoarenium  $\sigma$ -complex back to the EDA is simply taken as the microscopic reverse of its (rate of) formation. Although it is disfavored,<sup>38</sup> we cannot discount a direct (one-step) alternative suggested by a reviewer involving the heterolytic cleavage of the NO-arene bond.



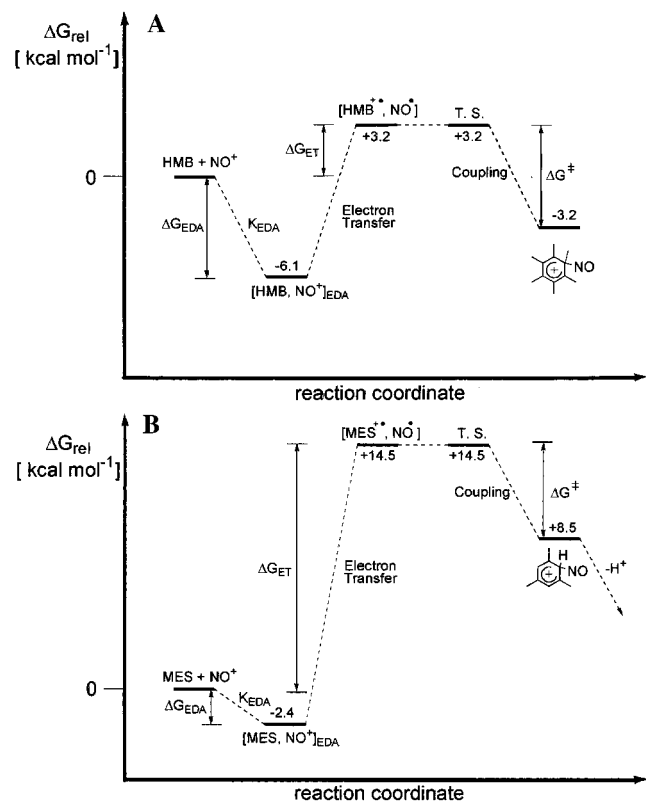


**Figure 10.** Energy diagrams for the reversible formation of (A) nitrosohexamethylbenzenium and (B) nitrosomesitylenium  $\sigma$ -complexes upon charge-transfer excitation of the EDA complexes of nitrosonium with the corresponding arenes. Diagram (B) represents the reaction energy profile for the thermal nitrosation of mesitylene by nitrosonium cation.

dependent equilibrium between nitrosoarenium and radical pair is “drained” by the escape ( $k_{\text{DISS}}$ ) of  $\text{ArCH}_3^{+\bullet}$  and  $\text{NO}^\bullet$  radicals out of the solvent cage of the radical pair to yield long-lived arene cation radicals. The rate of this process decreases with lowering of the temperature, and at the same time, the equilibrium of the formation of nitrosoarenium shifts toward the  $\sigma$ -complex. As a result, a decrease in the temperature leads to reduced amounts of long-lived cation radicals and predominant formation of nitrosoarenium  $\sigma$ -complexes with a slow decay kinetics.

**III. Energetics of the Formation of Nitrosoarenium.** On the basis of the reaction sequence in Scheme 3, the temperature dependence of the decay rate constants of nitrosoarenium (see Table 3), and the formation constants of the arene/ $\text{NO}^+$  EDA complexes determined previously,<sup>14,15</sup> we construct energy diagrams for the formation of nitrosoarenium as follows.

Let us first consider the reversible formation of nitrosoarenium ions derived from hexamethylbenzene and hexaethylbenzene (see Figure 10A). Both arenes form very strong EDA  $\pi$ -complexes with nitrosonium with formation constants of  $K_{\text{EDA}} = 31\,000$ <sup>14,15</sup> and  $K_{\text{EDA}} = 32\,500\text{ M}^{-1}$ ,<sup>41</sup> respectively, which corresponds to a formation free enthalpy of  $\Delta G_{\text{EDA}} \approx -6.1\text{ kcal mol}^{-1}$  relative to the uncomplexed arene and nitrosonium components ( $\Delta G_{\text{rel}} = 0$ ). On the other hand, electron transfer from (uncomplexed) hexamethylbenzene or hexaethylbenzene to nitrosonium, resulting in the formation of arene cation radical and nitric oxide, is endergonic by  $\Delta G_{\text{ET}} = 3.2\text{ kcal mol}^{-1}$  and  $\Delta G_{\text{ET}} = 2.5\text{ kcal mol}^{-1}$ , respectively, as

calculated from the differences between the oxidation potentials of the arenes and the reduction potential of nitrosonium.<sup>42</sup> Thus, the electron-transfer activation of the  $\text{NO}^+$   $\pi$ -complexes of hexamethylbenzene and hexaethylbenzene requires an energy of about  $9\text{ kcal mol}^{-1}$ , not considering any additional energies required for structural and solvent reorganization accompanying the electron-transfer process. In our time-resolved and steady-state photolysis experiments, this energy required for the formation of the radical pair is provided by light.

The subsequent collapse of the radical pair [ $\text{ArH}^{+\bullet}, \text{NO}^\bullet$ ] to the nitrosoarenium obviously does not require much activation energy, as judged from the ultrafast rate constant of this reaction step,<sup>43</sup> and we therefore locate the transition state (TS) for nitrosoarenium formation in first approximation on a comparable energy level to the radical-pair state. Since the decay and formation of the nitrosoarenium are reversible processes that occur via the same intermediates (see Scheme 3),<sup>38</sup> the energy level of the nitrosoarenium species can now be calculated using the activation free enthalpies ( $\Delta G^\ddagger$ ) of its decay. In other words, the difference between the free enthalpy of the transition state (TS) and that of nitrosoarenium can be equated to the activation free enthalpy ( $\Delta G^\ddagger$  in Table 3) for the decay of the latter, which amounts to  $6.4$  and  $3.7\text{ kcal mol}^{-1}$  for hexamethylbenzene and hexaethylbenzene, respectively. Thus, on the basis of the complete free energy diagram in Figure 10A, we conclude that the formation of nitrosohexamethylbenzenium is overall exergonic by  $3.2\text{ kcal mol}^{-1}$  relative to the uncomplexed starting materials (HMB and  $\text{NO}^+$ ); however, it is *endergonic* by about  $2.9\text{ kcal mol}^{-1}$  relative to the  $\text{HMB}/\text{NO}^+$  complex. Similarly, the formation of nitrosohexaethylbenzenium is exergonic by about  $1\text{ kcal mol}^{-1}$  relative to uncomplexed hexaethylbenzene and nitrosonium; however, its formation from the EDA complex is about  $5\text{ kcal mol}^{-1}$  *endergonic*. In other words, the  $\pi$ -complexes of both hexamethylbenzene and hexaethylbenzene with nitrosonium represent thermodynamic sinks of the reaction cycle due to their unusually high formation constants of  $K \approx 30\,000\text{ M}^{-1}$ .<sup>14,15,39</sup>

For mesitylene, the energy diagram is qualitatively similar to that of hexamethylbenzene; however, the relative energy levels of the various reactive intermediates are shifted (see Figure 10B). Thus, the EDA  $\pi$ -complex with nitrosonium is much less stabilized ( $\Delta G_{\text{EDA}} = -2.4\text{ kcal mol}^{-1}$ ), and the electron transfer from mesitylene to nitrosonium is strongly endergonic by  $14.5\text{ kcal mol}^{-1}$ .<sup>44</sup> Taking an activation free enthalpy for the decay of nitrosomesitylenium  $\sigma$ -complex similar to that of hexamethylbenzene (about  $6\text{ kcal mol}^{-1}$ ), we calculate its formation free energy to be  $+8.5\text{ kcal mol}^{-1}$  relative to uncomplexed mesitylene and nitrosonium, and about  $+11\text{ kcal mol}^{-1}$  relative to the mesitylene/ $\text{NO}^+$   $\pi$ -complex. This overall strongly *endergonic* formation of the Wheland intermediate in the nitrosation of mesitylene as well as the even more endergonic electron transfer that precedes the formation of this  $\sigma$ -complex causes the pair of equilibria in Scheme 3 to lie far on the side of the starting materials, viz., the mesitylene/ $\text{NO}^+$  complex. Thus, it is the (one-way) deprotonation of the Wheland

(42) The oxidation potentials of HMB and HEB are  $1.62$  and  $1.59\text{ V}$  vs SCE in dichloromethane, respectively. (See: Howell, J. O.; Goncalvez, J. M.; Amatore, C.; Klasinc, L.; Wightman, R. M.; Kochi, J. K. *J. Am. Chem. Soc.* **1984**, *106*, 3968.) The reduction potential of nitrosonium is  $1.48\text{ V}$  vs SCE in dichloromethane. (See: Lee, K. Y.; Kuchynka, D. J.; Kochi, J. K. *Inorg. Chem.* **1990**, *29*, 4196.) This approximate determination of  $\Delta G_{\text{ET}}$  does not include any inner-sphere component to electron-transfer.

(43) Rate constants of  $k > 10^{11}\text{ s}^{-1}$  approach those of barrier-free reactions. See ref 27, p 173.

(44) (a) The formation constant for mesitylene/ $\text{NO}^+$  complexes is  $K_{\text{EDA}} = 56\text{ M}^{-1}$ .<sup>14,15</sup> (b) The oxidation potential of mesitylene is  $2.11\text{ V}$  vs SCE in dichloromethane.<sup>41</sup>

(41) Rathore, R.; Lindeman, S. V.; Kochi, J. K. *J. Am. Chem. Soc.* **1997**, *119*, 9393.

intermediate which slowly pulls the highly endergonic reaction equilibria toward the final nitrosomesitylene product.<sup>45</sup>

### Summary and Conclusions

The time-resolved spectroscopy experiments described in this work lead to the real-time observation of the formation and decay of nitrosoarenium  $\sigma$ -complexes upon charge-transfer photoexcitation of the EDA complexes of nitrosonium cation with various arenes. For mesitylene and *p*-xylene, which are both nitrated by nitrosonium,<sup>14</sup> these results represent the first direct observation of true Wheland intermediates in electrophilic aromatic substitution. The lifetimes of the nitrosoarenium  $\sigma$ -complexes are found to depend strongly on the temperature and vary from nanoseconds at room temperature in solution to hours at  $T = 77$  K in a butyl chloride glass. Femtosecond laser experiments reveal the ultrafast formation ( $k \approx 10^{11} \text{ s}^{-1}$ ) of the nitrosoarenium  $\sigma$ -complexes by radical-radical coupling of arene cation radical with nitric oxide, which confirms the electron-transfer mechanism for electrophilic aromatic nitrosations proposed previously.<sup>14</sup> Based on this reaction scheme and the kinetic and thermodynamic data obtained in this study, energy diagrams are constructed which establish the highly endergonic reaction profile of electrophilic aromatic nitrosations and thus explain the low efficiency of aromatic nitrosations as compared to the corresponding nitration reactions.<sup>10</sup>

### Experimental Section

**Materials.** Hexamethylbenzene (Acros), hexaethylbenzene (Acros), pentamethylbenzene (Aldrich), durene (Aldrich), and dimethoxybenzene (Aldrich) were recrystallized from ethanol. Mesitylene and *p*-xylene (Aldrich) were purified by distillation. The synthesis and purification of TMT<sup>39</sup> and TET<sup>39</sup> (see Table 2, entries 3 and 4, respectively),

(45) (a) The endergonic equilibria which are slowly drained by deprotonation explain not only the sluggish rates of thermal nitrosations but also the fact that photonitrosations are extremely inefficient.<sup>14</sup> (b) Recently, energy diagrams for aromatic nitrosations (such as in Figure 10) have been reported based on ab initio MO and Hartree-Fock/density functional calculations.<sup>45c</sup> All theoretical treatments uniformly predict an initial, barrier-free formation of arene/NO<sup>+</sup> EDA complexes. However, there are conflicting results about the Wheland intermediate, viz., nitrosoarenium, which—depending on the method and level of the calculation—is obtained either as a more or less stable minimum or as a saddle point (transition state) between the EDA complex and N-protonated nitrosobenzene. Our experimental results reported here support the CISD/6-31G(d) calculations which predict a large energy barrier for the conversion of the  $\sigma$ -complex to an N-protonated nitrosobenzene and thus identify the deprotonation of the Wheland intermediate as the rate-determining step. (c) Shokov, S.; Wheeler, R. A. *J. Phys. Chem.* **1999**, *103*, 3A, 4261.

hexaphenylbenzene,<sup>46</sup> dimethoxydurene,<sup>47</sup> CRET (see Table 4, entry 3),<sup>48</sup> 2-methoxybiphenyl,<sup>46</sup> and the hindered naphthalene (see Table 4, entry 5)<sup>49</sup> have been described previously. Dichloromethane, *n*-chlorobutane, acetonitrile, and chloroform were purified according to standard laboratory procedures.<sup>50</sup>

**Instrumentation.** Steady-state absorption spectra were obtained using a Hewlett-Packard 8453 diode-array spectrophotometer. For the low-temperature measurements, the spectrophotometer was equipped with a quartz dewar filled with either liquid nitrogen or acetone/dry ice mixtures. The nanosecond/microsecond time-resolved absorption spectra were recorded using the second (532 nm) or third (355 nm) output of a 10-ns Q-switched Nd:YAG laser (Continuum) as excitation source and a kinetic spectrometer equipped with a quartz dewar described in detail elsewhere.<sup>51</sup> The picosecond time-resolved measurements were carried out with a pump-probe spectrometer using the second (532 nm) and third (355 nm) output of a 25-ps mode-locked Nd:YAG laser (Continuum) as excitation source.<sup>51</sup> For the sub-picosecond time-resolved measurements, a Ti:sapphire laser system (Photonics Instruments) was used consisting of a Ti:sapphire oscillator and two Ti:sapphire amplifiers.<sup>23c</sup> The oscillator is pumped by an argon ion laser (Coherent) to generate 110-fs laser pulses at 400 nm. The nanojoule pulses are amplified sequentially by a regenerative amplifier and a linear (multipass) amplifier, both of which are pumped by a frequency-doubled (532 nm), Q-switched Nd:YAG laser (Continuum, 10 ns, 10 Hz). The laser system generates 230-fs laser pulses with an energy of 10 mJ at 800 nm. The frequency-doubled output (400 nm, 3 mJ) was used as excitation source.<sup>23c</sup>

**Preparation of Arene/NO<sup>+</sup> Complexes.** The EDA complexes of nitrosonium with arenes were prepared by adding millimolar concentrations of arene to a suspension of NO<sup>+</sup>BF<sub>4</sub> in dichloromethane or *n*-butyl chloride, respectively. The mixture was stirred until a brown color appeared and the characteristic spectrum of the arene/NO<sup>+</sup> complex could be recorded. The residual undissolved nitrosonium salt was removed and the concentration of the homogeneous solution adjusted to obtain absorbances between 0.5 and 1.0 at the excitation wavelength (355, 400, or 532 nm).

**Acknowledgment.** We thank R. Rathore for many helpful discussions and for providing the methoxy-substituted and the hindered aromatic compounds, and the National Science Foundation and the R. A. Welch Foundation for financial support.

JA001318U

(46) Rathore, R., unpublished results.

(47) Rathore, R.; Bosch, E.; Kochi, J. K. *Tetrahedron* **1994**, *50*, 6727.

(48) Rathore, R.; Kochi, J. K. *J. Org. Chem.* **1995**, *60*, 4399.

(49) Rathore, R.; Kochi, J. K. *Acta Chem. Scand.* **1998**, *52*, 114.

(50) Perrin, D. D.; Armarego, W. L. F.; Perrin, D. R. *Purification of Laboratory Chemicals*, 2nd ed; Pergamon: New York, 1980.

(51) Bockman, T. M.; Kochi, J. K. *J. Chem. Soc., Perkin Trans. 2* **1996**, 1633.